FACTA UNIVERSITATIS
Series: **Mechanical Engineering**
https://doi.org/10.22190/FUME220114015M

Original scientific paper

WEAR LOAD CAPACITY OF CROSSED HELICAL GEARS

Aleksandar Miltenović[1], Milan Banić[1], Jovan Tanasković[2], Jelena Stefanović-Marinović[1], Damjan Rangelov[1], Marko Perić[1]

[1]Unversity of Niš, Faculty of Mechanical Engineering, Serbia
[2]University of Belgrade, Faculty of Mechanical Engineering, Serbia

Abstract. *The paper presents a wear load capacity of crossed helical gears (gear pair consists of a worm and a helical gear). Crossed helical gears are similar to worm gear pairs, and it is logical to extend the load capacity calculation approach of worm gears for the case of crossed helical gears. One of the disadvantages of crossed helical gear sets is very high running-in wear. The paper explains the transition between running-in and steady-state wear and proposes a joint wear calculation model. The paper outlines a proposal to extend the calculation method for wear load capacity from a worm gear pair to the case of crossed helical gears (a worm with a helical gear). This calculation method for determining the wear load capacity of crossed helical gears is verified for the cases when the wheel is of bronze CuSn12Ni2-C-GCB and sintered steel Fe1.5Cr0.2Mo.*

Key Words: *Crossed Helical Gears, Wear, Bronze, Sintered Steel, Load Capacity*

1. INTRODUCTION

Gears belong to the group of the most common parts used for power transmission in various types of machines [1, 2, 3]. They are exposed to cycles of normal and shear forces that give rise to wear. As one of the most important limiting factors for the lifetime of gears, wear load capacity needs to be given a special attention. Gear tooth surface wear is common in the gears together with bending fatigue, pitting, micropitting and scuffing. Wear for crossed helical gears is the most common damage since the contact between the gear teeth is of a 'point type', which is disadvantageous compared to other gear types that have a so-called 'line contact'. Crossed helical gears are less researched than the other gear types since they have lower load capacity, and, therefore, industry did not show greater interest in investigating them. Mostly, industry application is of the crossed helical

*Received: January 14, 2022 / Accepted March 25, 2022
Corresponding author: Aleksandar Miltenović
University of Niš, Faculty of Mechanical Engineering, A. Medvedeva 14, 18000 Niš, Serbia
E-mail: aleksandar.miltenovic@masfak.ni.ac.rs

gears with a smaller size that do not need to have higher load capacity. The application primarily transmits some lower power and motion like in actuators and auxiliary drives. The advantage of crossed helical gears is that their assembling is much easier and does not affect their operation characteristics compared with worm gears. For the proper operation of worm gear drives and achievement of prescribed values of load capacity is necessary to have precise assembling of the worm wheel.

Wear for gears is described, in literature, as the process of continuous removal of surface material from tooth flank. In the case of crossed helical gears, removal is intensified initially since running-in wear is in the circumstance of contact in point. Running-in is followed by steady-state wear where wear rates are lower since the contact is now in the line that is growing with the progression of wear. Vullo [4, 5] gave a review of state of the art for wear generation mechanism and crossed helical gears kinematics. He showed different approaches in calculating gear wear like Hertz theory, Holm's, and Archard's wear calculation method for wear linear progression. Shilko [6] used an advanced discrete-element-based mechanical model for modeling wear of ductile materials that considers fracture and surface adhesion. Cao [7] proposed fracture-induced adhesive wear criterion. The idea of the wear criterion is to predict the wear process of a mixed lubricated point contact in sliding motion that can be used in the simulation. He compared simulation and experiment measurements that had a reasonable agreement. Wagner [8] studied the effect of contact pressure and surface texture on the running-in behavior in the case of carburized steel under boundary lubrication. He demonstrated running-in of the surface within one thousand load cycles "regardless of the pressure or initial composite surface roughness".

VDI 2736-3 [9] provide load capacity calculation for crossed helical gear sets with material combination steel and plastics. DIN 3996 [10] provides the calculation of the load capacity of cylindrical worm gear pairs with rectangular crossing axes. One of the calculations is for wear load capacity. Wendt [11] investigated load capacity for worm with helical gear set combination steel/sintered steel. He used sintered steel Fe1.5Mo0.3C with different material density where he proved that increased material density brings higher wear resistance. In addition, he provides approximate equations for the calculation of safety factors for wear and pitting. Boehme [12] presented a calculation method for crossed helical gears with optimized Hertzian contact pressures and sliding paths that are designed to increase the load capacity. Norgauer [13] presented the calculation and simulation for the design of crossed helical gear sets. Simulation is integrated into software SCHRAD2 to calculate contact patterns without and under load. For under load conditions, he determined the stiffness of the gearbox. Liang [14] proposed a generation approach of gear pair with small-angle based on the curve contact element to improve load capacity and transmission characteristics of crossed-axis helical gear drive. He introduced spatial curve meshing relationships for contact principle. He also produced a prototype and carried out basic tests that show well contact characteristics.

The load capacity of worm gears has been developed over a long period on standards based on industrial experience, and they were published in DIN 3996. ISO TR 14521 Standard – Calculation of Load Capacity of Worm Gears is based on DIN 3996. Wear is one of the typical damages for worm gears, and it usually appears on the tooth flanks of worm wheels [15]. Chernets [16] presented the computation method of studying worm gears with Archimedean and involute worm. He showed that the correction coefficient of wheel teeth decreases maximal contact pressures and the wear of wheel teeth.

Daubach [17] developed a simulation model for the abrasive wear of worm gears based on the energetic wear equation. This simulation model includes a tooth contact analysis and tribological calculation to determine friction and wear. Ivanov [18] analyzed the wear of worm gears in the running-in operation. He showed that wear in the running-in phase in uniform over the gear width influences efficiency, and after the running-in stage is recommendable to replace the lubricant. Also, in the running-in phase, variations of load and velocity are undesirable.

Weisel [19] researched experimentally a worm with a helical gear wheel. He demonstrates that the load capacities of crossed helical gear sets after the running-in phase are like worm gears. Miltenovic [20, 21, 22] investigated the wear resistance of worm with helical gear set combination steel/sintered steel where he used Fe1.5Cr0.2Mo with different additional treatments. Sintered steel Fe1.5Cr0.2Mo is an interesting material with good wear resistance characteristics, suitable for mass production, while sinter-hardening treatment had the best wear resistance characteristics. Krol [23] investigated the parameters of worm gearing with increased wear resistance in the specific application. As a result, he succeeded in influencing the wear rates by changing the basic parameters of the gear set.

The novelty of this paper lies in a calculation approach for the wear load capacity of crossed helical gears in applications that are like worm gears. As there is a high geometrical similarity between these two gear pairs, it is logically possible to use the basics of the wear load capacity calculation of worm gears for the case of crossed helical gears. For this approach, verification is performed in an experiment and the calculation validates this method. The investigation is conducted for two materials: bronze CuSn12Ni2-C-GCB and sintered steel Fe1.5Cr0.2Mo with sinter-hardening treatment. Bronze CuSn12Ni2-C-GCB is the standard material for worm wheel, and it covers with necessary data for load capacity calculation according to DIN 3996.

2. TEST CONDITIONS

Experiments have been carried on test benches with center-to-center distance of 30 mm. On the input side of the transmission is on-worm-mounted asynchronous motor, and on the output side, on the wheel is connected with a magnetic particle brake. The torque measurement system is mounted on the input and output sides, and measurement was made with a torque gauge bar *via* a slip ring transmitter. The crossed helical gear set data is given in Table 1, and the test bench is presented in Fig. 1.

The wear resistance of crossed helical gears is investigated for input speeds of 1500, 5000 and 10000 min^{-1}. At the beginning of the test, output torque is 12 Nm for speeds of 1500 and 5000 min^{-1} and 8 Nm for 10000 min^{-1}. After 40h, output torque was increased by 4 Nm up to the maximal output torque that these crossed helical gears can resist. Every test was repeated three times. Measurement of wear depth was carried out every 20 h at Klingerberg PNC 65 measuring machine.

Module *m* of the bronze gears is 1.25 mm while for sintered steel gears is 1.252 mm, which is the consequence of material increase during the sintering process. The test equipment is better explained in [24].

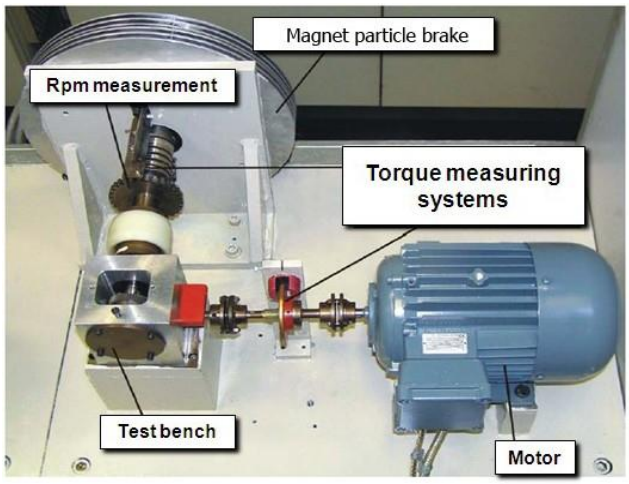

Fig. 1 Test bench

Table 1 Data of the test gear pair

Parameter	Data	
	worm	wheel
Center distance	30 mm	
Shape of worm flank	ZI	
Module	1.25 (1.252) mm	
Transmission ratio	40	
Number of teeth	1	40
Pressure angle	20°	
Profile shift coefficient	0	
Lead direction	left	
Gear width	25 mm	10 mm
Helix angle at reference circle	82.493°	7.507°
Reference diameter	9.57 mm	50.43 mm
Tip diameter	12.09 mm	52.95 mm
Root diameter	6.54 mm	47.41 mm
Transverse contact ratio	1.852	
Material	Fe1.5Cr0.2Mo CuSn12Ni2-C-GCB	16MnCr5
Input speed	1500, 5000 and 10000 min^{-1}	
Output torque	12–36 Nm for 1500 and 5000 min^{-1} 8–20 Nm for 10000 min^{-1}	
Number of starts	1 per 20h	
Lubrication	Oil Klüber GH6 1500	

3. CALCULATION METHOD

Wear describes the loss of material from the surface in the contact. In the case of gears, this leads to a reduction of the tooth thickness. According to DIN 3996, wear load capacity is determined with safety factor against wear S_W calculated from the permissible wear on flank δ_{wlimn} and wear depth δ_{wn} in (n) normal section (1).

$$S_W = \delta_{w\lim n} / \delta_{wn} \geq S_{W\min} = 1.1 \tag{1}$$

Wear depth δ_{wn} is based on experiments, and it depends on the material and lubricant combination that is used in tests. Wear depth directly defines wear resistance, and material and lubricant combinations with lower wear depth have greater wear resistance and higher wear load capacity. Wear depth δ_{wn} directly depends on wear intensity J_W and wear path s_{Wm} (2).

$$\delta_{wn} = J_W \cdot s_{Wm} \tag{2}$$

Wear intensity J_W depends on basic wear intensity J_{0T} for the specific material and factors that bring closer basic wear intensity and specific operation characteristics. According to DIN 3996 [10], wear intensity J_W - Eq. (3) depends on material lubrication factor $W_{ML,}$ which values are given in the appropriate Table and the factor for starts W_{NS} that is calculated by proper equitation defined in the standard [10].

$$J_W = J_{0T} \cdot W_{ML} \cdot W_{NS} \tag{3}$$

W_{ML} values depend on lubrication and material of worm wheel and are limited only to some materials. This means that for material Fe1.5Cr0.2Mo would be impossible to choose the value for this factor. The factor for starts W_{NS} considers the influence of repeated starts on wear and can be determined by Eq. (4), depending on the number of starts/hour N_S.

$$W_{NS} = 1 + 0.015 \cdot N_S \leq 3 \tag{4}$$

Wendt [11], in his research, proposed Eq. (5), where he introduced material factor $Y_{T\rho}$ that considers material density without using W_{ML} and W_{NS}. In this case, the introduction of the material factor is logical since he used the same sintered materials for the gear wheel with different material densities (6.9 and 7.2 kg/dm3) in his research.

$$J_W = J_{0T} \cdot Y_{T\rho} \tag{5}$$

The authors of this paper choose not to use W_{NS}, $W_{ML,}$ and $Y_{T\rho}$ because of the following reasons:

- W_{ML} – material lubrication factor is practically unusable for these materials, and it has only character of simple magnification that does not affect character of wear progression by crossed helical gear.
- W_{NS} – factor for number of starts does not have influence in the test case since its value would be 1.00075 and specific test for this factor are not carried out. There is a possibility for this factor to be used in the case of crossed helical gear set in the form of Eq. (4) or some other form, but additional tests are necessary.

- $Y_{T\rho}$ – material factor is unsuitable since there are no same materials with different densities.

According to the tests for crossed helical gears, authors propose that wear intensity J_W (Eq. (6)) depends on basic wear intensity and crossed helical factor W_{SR} where crossed helical factor W_{SR} include specific character of wear progression for crossed helical gear set.

$$J_W = J_{0T} \cdot W_{SR} \tag{6}$$

According to experiments presented in Section 4, basic wear intensity J_{0T} has values for bronze CuSn12Ni2-C-GCB and sintered steel Fe1.5Cr0.2Mo that can be calculated with Eq. (7).

$$J_{0T} = B_1 \cdot K_W^{B_2} \tag{7}$$

Table 2 Data of the test gear pair

Material	Coefficient	
	B_1	B_2
Fe1.5Cr0.2Mo sinter-hardening	320.5×10^{-9}	-0.355
CuSn12Ni2-C-GCB	143×10^{-8}	-0.74

Characteristic value for lubrication gap K_W is calculated according to DIN 3996, and it gives connections with load, size, materials, etc. Coefficients B_1 and B_2 for bronze CuSn12Ni2-C-GCB and sintered steel Fe1.5Cr0.2Mo with sinter-hardening treatment are shown in Table 2.

Table 3 Coefficients of Eq. (8)

Material	Coefficient		
	A_1	A_2	A_3
Fe1.5Cr0.2Mo sinter-hardening	-0.05359	$3.57093\text{x}10^{-4}$	$-2.92964\text{x}10^{-8}$
CuSn12Ni2-C-GCB	-0.21911	$3.42276\text{x}10^{-4}$	$-1.98877\text{x}10^{-8}$

Crossed helical gears factor W_{SR} – Eq. (8) includes the wear increase during the running-in period and regular operation of the crossed helical gear set. It depends on lifetime L_h and input speed n_1 and experimentally determined coefficients A_0, A_1 and A_2 given in Table 3 for bronze CuSn12Ni2-C-GCB and sintered steel Fe1.5Cr0.2Mo.

$$W_{SR} = \frac{(\log L_h)^{0.02}}{L_h} \cdot \frac{1}{\left(A_0 + A_1 \cdot n_1 + A_2 \cdot n_1^2\right)} \tag{8}$$

Eq. (8) is proposed by the authors because it follows the character of wear progression of crossed helical gear set and it can be used for rotation speed $n_1 > 1500$ min^{-1} and $n_1 < 10000$ min^{-1}. The crossed helical gears factor can be determined only experimentally.

4. VERIFICATION OF THE CALCULATION METHOD

Due to its geometry, a crossed helical gear has two phases during operation: the running-in phase and the regular operation that comes after the running-in phase.

Fig. 2 shows the comparison of teeth flanks of crossed helical gears made from sintered steel Fe1.5Cr0.2Mo and CuSn12Ni2-C-GCB for input speed n_1 = 5000 min^{-1} and different output torque from 12 to 32 Nm.

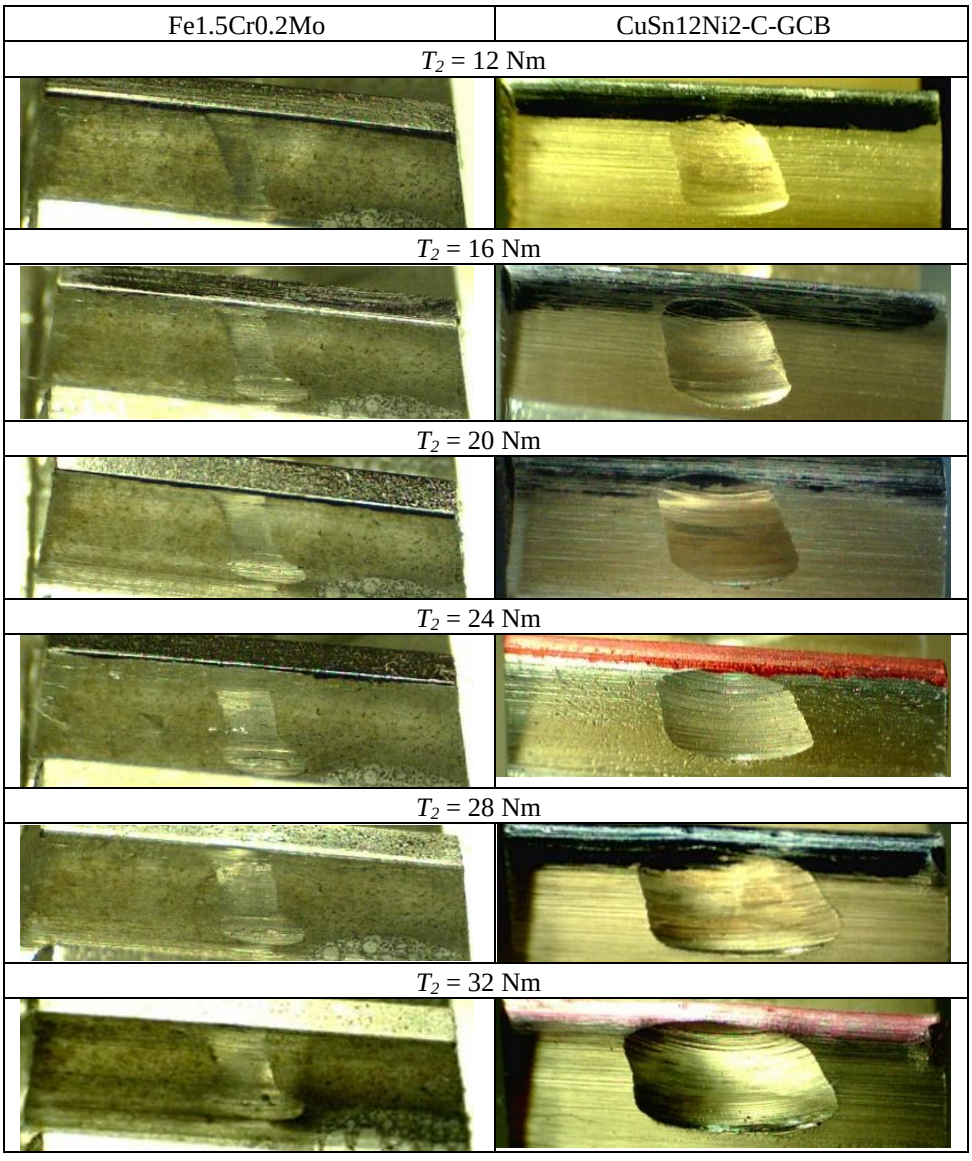

Fig. 2 Comparison of wear at teeth flanks of crossed helical gears for input speed n_1 = 5000 min^{-1} and different output torque

Every helical gear is measured at reference diameter on Klingelberg PNC 65 after 20h long test. Each measurement was performed on three teeth, which are located approx. at 120^o and the value of wear depth that is used in further research is an average value of wear depth at three teeth. Example of measurement protocol is given in Fig. 3.

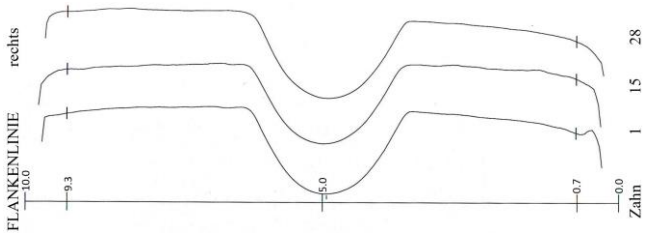

Fig. 3 Measurement protocol for measuring wear depth of helical gear

4.1 Wear during the running-in phase

The running-in wear occurs immediately at the beginning of the operation due to the high flank pressure at the contact point. The running-in wear is a complex process, and, in some cases, running-in wear rates can be relatively large for such a short operation time. Since the contact, in the beginning, is at a point and there is no oil between the flanks, the direct steel-to-steel contact occurs. This can lead to short scuffing or very high abrasive wear due to a direct steel-to-steel contact, which is followed by lower wear rates with the lubrication film.

Fig. 4 shows wear depth δ_{wn} for different input rotation speeds and identical load and operation time.

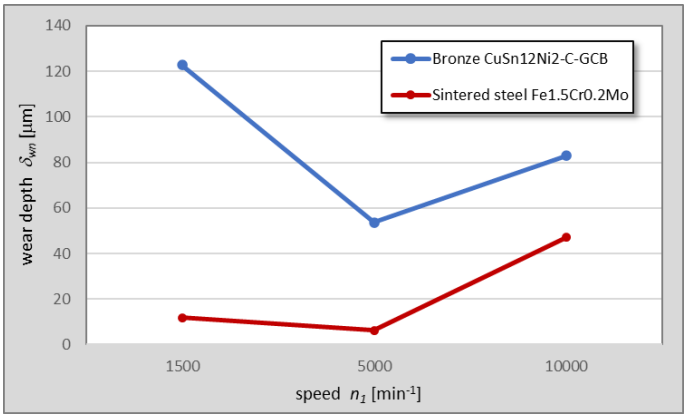

Fig. 4 Running-in wear for speed n_1= 1500, 5000 and 10000 min^{-1} for output torque 12 Nm and operation time 20 h

Scuffing is a specific damage form and compared with wear it is much more dangerous for the flanks. The scuffing load capacity is not sufficiently explored yet to specify standardized calculation. Temporarily occurring scuffing damage to bronze

wheels can be "healed" again. This healing is possible only through wear, but it cannot currently be considered in estimating the wear life of the DIN 3996 standard. Scuffing depends significantly on the material in contact, and it is much more unstable to predict than wear. This means that running-in wear can encompass short running-in scuffing.

Rotation speed plays a significant role and has a dual influence on running-in wear.

1. The thickness of the lubrication film depends directly on the speed, and with an increase in the rotation speed, the lubrication film thickness also rises. A higher lubrication film thickness decreases the running-in wear. This means that the running-in wear could be lower at high speeds.
2. A higher speed increases the working temperature, decreasing the viscosity of oil and increasing the running-in wear. This means that the running-in wear could increase more at high speeds.

The lowest wear depth is for the speed of n_1 = 5000 min^{-1} in both cases. Bronze has a higher wear rate for all speeds, and its running-in wear is higher for n_1 = 1500 min^{-1} than for n_1 = 10000 min^{-1}. This process is followed by an increase in the contact line and a decrease in the contact pressure. Therefore, running-in wear is the lowest in the case of n_1 = 5000 min^{-1} for both materials. This means that scuffing in the running-in wear phase is the smallest or does not exist at a speed of n_1 = 5000 min^{-1}.

After the running-in phase comes to the operation with an approximately constant increase in wear depth δ_{wn}. The worm acts like a cutter that creates a globoid flank and spreads contact from the contact point to the contact in line that grows as the wear depth grow. Fig. 5 compares the calculated (Eq. 2) and the measured wear depths during the running-in process for bronze CuSn12Ni2-C-GCB and sintered steel Fe1.5Cr0.2Mo.

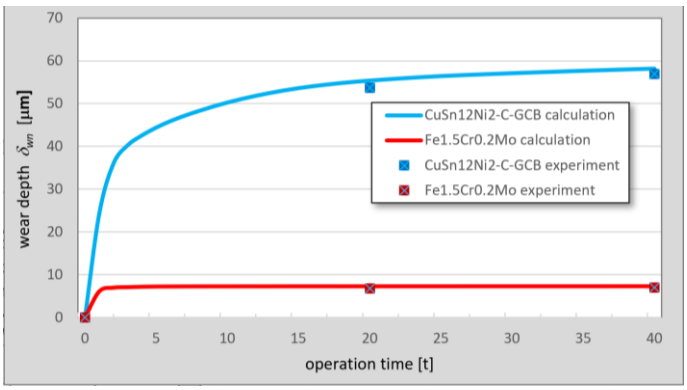

Fig. 5 Experimental and calculation results for running-in wear

4.2 Experimental results

Figs. 6 to 11 represent the comparison of calculated and measured values of wear depth δ_{wn} for the helical gear made of sintered steel Fe1.5Cr0.2Mo with sinter-hardening treatment and CuSn12Ni2-C-GCB and for input speeds of n_1 = 1500, 5000 and 10000 min^{-1}. The results at the input speed n_1 = 5000 min^{-1} are more stable than with n_1 = 1500 and 10000 min^{-1} and due to the running-in wear phase issue and dual influence of rotation speed are explained in 4.1.

Fig. 6 shows a comparison of calculated and measured wear depth δ_{wn} for the helical gear made of CuSn12Ni2-C-GCB for n_1 =1500 min^{-1}. Bronze has a highest running-in wear for n_1 = 1500 min^{-1}.

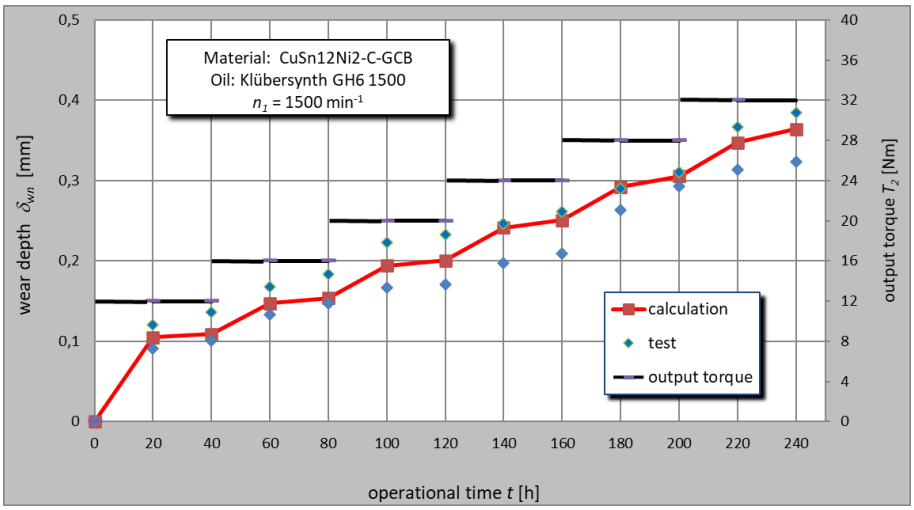

Fig. 6 Calculated and measured wear rates δ_{wn} for the helical gear made of CuSn12Ni2-C-GCB for n_1 =1500 min^{-1}

Fig. 7 shows a comparison of calculated and measured wear rates δ_{wn} for the helical gear made of CuSn12Ni2-C-GCB for n_1 =5000 min^{-1}. In this case, the values of wear rate are most minor and repeatability gave the best repetition of results.

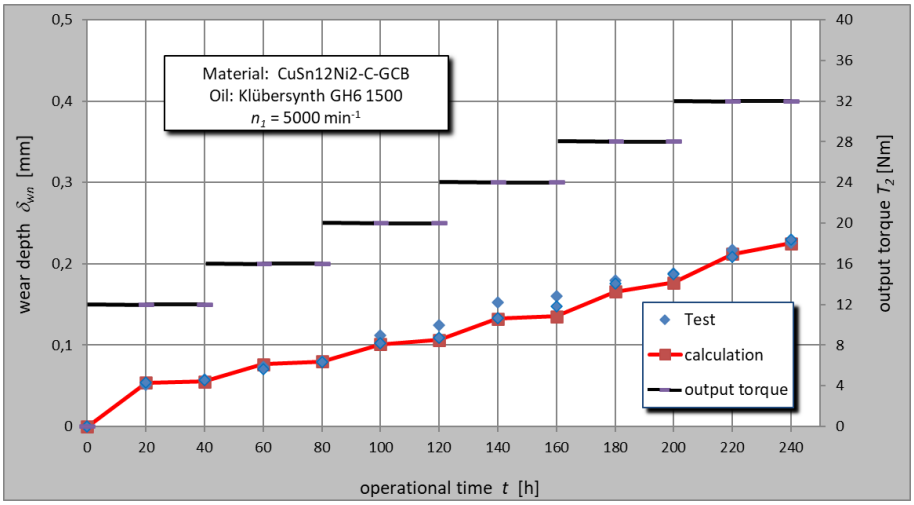

Fig. 7 Calculated and measured wear rates δ_{wn} for the helical gear made of CuSn12Ni2-C-GCB for n_1 =5000 min^{-1}

Fig. 8 shows a comparison of calculated and measured wear rates δ_{wn} for the helical gear made of CuSn12Ni2-C-GCB for n_1 =10000 min^{-1}.

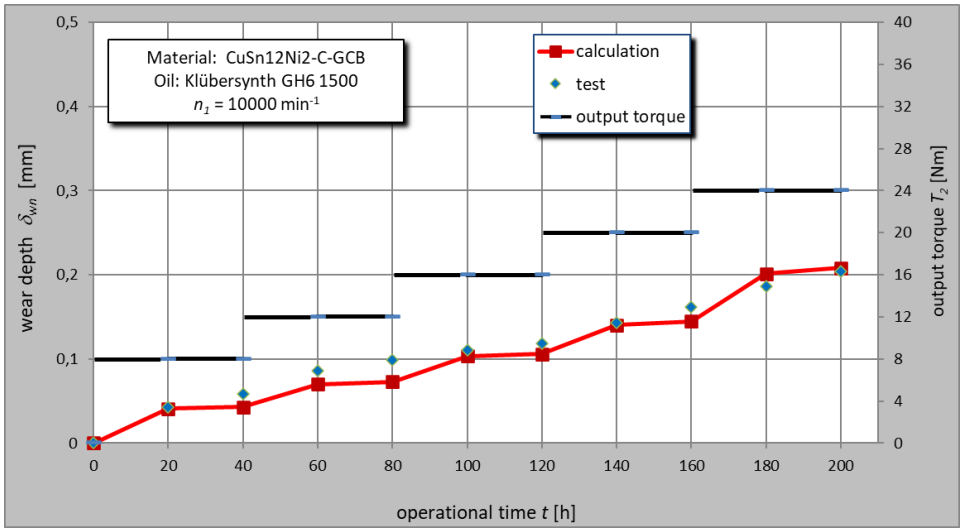

Fig. 8 Calculated and measured wear rates δ_{wn} for the helical gear made of CuSn12Ni2-C-GCB for n_1 = 10000 min^{-1}

Fig. 9 shows a comparison of calculated and measured wear rates δ_{wn} for the helical gear made of Fe1.5Cr0.2Mo for n_1 =1500 min^{-1}.

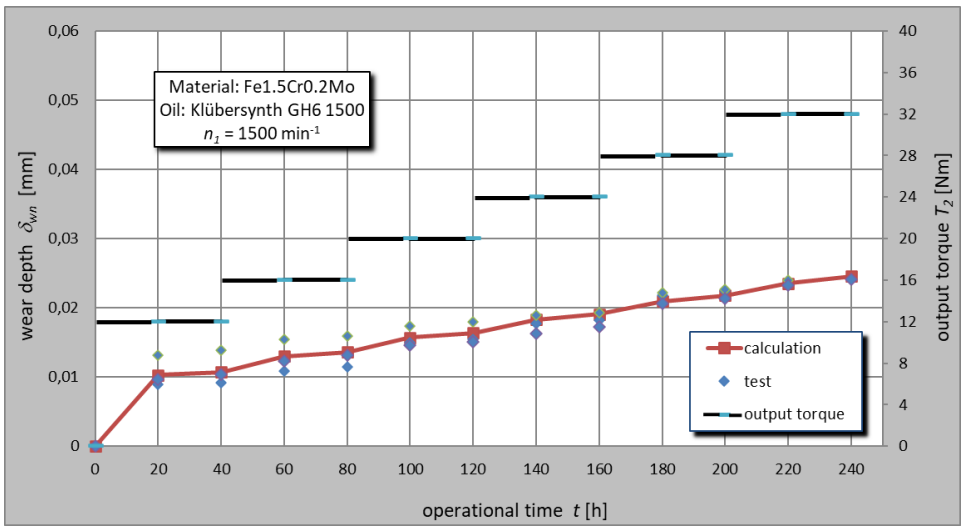

Fig. 9 Calculated and measured wear rates δ_{wn} for the helical gear made of Fe1.5Cr0.2Mo for n_1 =1500 min^{-1}

Fig. 10 shows a comparison of calculated and measured wear rates δ_{wn} for the helical gear made of Fe1.5Cr0.2Mo for n_1 =5000 min^{-1}.

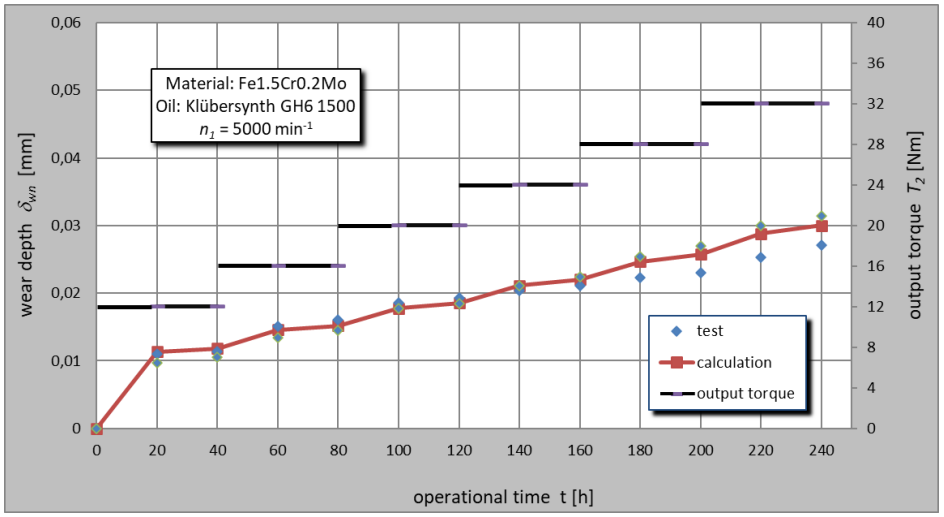

Fig. 10 Calculated and measured wear rates δ_{wn} for the helical gear made of Fe1.5Cr0.2Mo for n_1 =5000 min^{-1}

Fig. 11 shows a comparison of calculated and measured wear rates δ_{wn} for the helical gear made of Fe1.5Cr0.2Mo for n_1 =10000 min^{-1}. Sintered steel has a highest running-in wear for n_1 = 10000 min^{-1}.

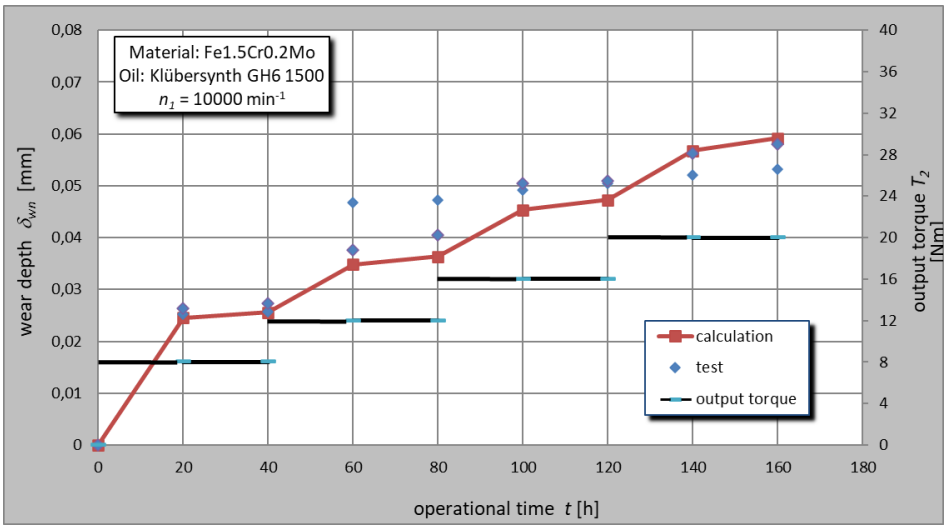

Fig. 11 Calculated and measured wear rates δ_{wn} for the helical gear made of Fe1.5Cr0.2Mo for n_1 = 10000 min^{-1}

5. CONCLUSIONS

This paper presents the experimental and theoretical results of the worm with the helical gear made of bronze CuSn12Ni2-C-GCB and sintered steel Fe1.5Cr0.2Mo with sinter-hardening treatment.

The running-in wear is a complex process that occurs immediately at the beginning of the operation due to the high flank pressure at the contact point. Since the contact, in the beginning, is where there is no oil between the flanks, the direct steel-to-steel contact occurs. This can lead to short scuffing or very high abrasive wear due to the direct steel-to-steel contact, followed by lower wear rates with the lubrication film. Scuffing depends significantly on the materials in contact, and it is much more unstable to predict than wear. This means that running-in wear can encompass short running-in scuffing.

Rotation speed plays a significant role and has a dual influence on running-in wear. The thickness of the lubrication film depends directly on the speed, and an increase in the rotation speed decreases the running-in wear. On the other hand, higher speeds increase the working temperature, reducing the oil viscosity and increasing the running-in wear. For the running-in phase, the moment of transition from the non-oil film contact to the contact with the oil film is crucial. The lowest wear depth is for speed of n_1 = 5000 min^{-1} for both materials due to the dual influence on the running-in wear. Bronze has a higher wear depth for all speeds, and the bronze running-in wear is higher for n_1 = 1500 min^{-1} than for n_1 = 10000 min^{-1}.

The paper presents a calculation method for the wear load capacity of crossed helical gears in applications that are similar to worm gears. As there is a high geometrical similarity between these two gear pairs, the paper proposes a possible expansion of the wear load capacity calculation of worm gears to the case of crossed helical gears. It gives some form of guidelines for cases of crossed helical gears. For this purpose, the paper introduces coefficient W_{SR} that includes the wear progression during the running-in wear phase and after it; it depends on the material type, lifetime, and input speed. It can be determined only by experiment.

For this approach, verification is given in an experiment and the calculation that validates this method. This is done for two materials: bronze CuSn12Ni2-C-GCB and sintered steel Fe1.5Cr0.2Mo.

Acknowledgements: *This research was financially supported by the Ministry of Education, Science and Technological Development of the Republic of Serbia (Contract No. 451-03-9/2021-14/200109 and 451-03-9/2021-14/200105).*

REFERENCES

1. Xue, Q., Zhang, X., Geng, C., Teng, T., 2021, *Gear shift coordinated control strategy based on motor rotary velocity regulation for a novel hybrid electric vehicle*, Applied Sciences, 11(24), 12118.
2. Wang, A., Li, Y., Du, X., Zhong, C., 2021, *Diesel engine gearbox fault diagnosis based on multi-features extracted from vibration signals*, IFAC-PapersOnLine, 54(10), pp. 33-38.
3. Marinković, Z., Marinković, D., Petrović, G., Milić, P., 2013, *Modelling and simulation of dynamic behaviour of electric motor driven mechanisms*, Tehnicki Vjesnik, 19(4), pp. 717-725.
4. Vullo, V., 2020, *Gears - Volume 1: Geometric and Kinematic Design*, Springer Nature Switzerland AG, Switzerland.

5. Vullo, V., 2020, *Gears - Volume 2: Analysis of Load Carrying Capacity and Strength Design*, Springer Nature Switzerland AG, Switzerland.
6. Shilko, E., Grigoriev, A., Smolin, A., 2021, *A Discrete Element Formalism for Modelling Wear Particle Formation in Contact Between Sliding Metals*, Facta Universitatis-Series Mechanical Engineering, 19(1), pp. 7-22.
7. Cao, H., Tian, Y., Meng, Y., 2021, *A Fracture-Induced Adhesive Wear Criterion and Its Application to the Simulation of Wear Process of the Point Contacts under Mixed Lubrication Condition*, Facta Universitatis-Series Mechanical Engineering, 19(1), pp. 23-38.
8. Wagner, J.J., Jenson, D.A., Sundararajan, S., 2017, *The effect of contact pressure and surface texture on running-in behavior of case carburized steel under boundary lubrication*, Wear, 376-377, pp. 851–857.
9. VDI 2726 2736 Blatt 3, 2012, *Thermoplastische Zahnräder, Schraubradgetriebe, Paarung Zylinderschnecke Schrägstirnrad, Tragfähigkeitsberechnung*, Beuth Verlag, Berlin.
10. DIN 3996: *Tragfähigkeitsberechnung von Zylinder-Schneckengetrieben mit sich rechtwinklig kreuzenden Achsen*, 2012.
11. Wendt, T., 2008, *Tragfähigkeit von Schraubradgetrieben mit Schraubrädern aus Sintermetall*, Dissertation Ruhr-Universität Bochum.
12. Boehme, C., Vill, D., Tenberge, P., 2019, *Enhanced application limits for crossed helical gearboxes using new geometries for smaller sliding paths or smaller contact pressures*, Power transmission 2019, MATEC Web of Conferences, 287, 01010.
13. Norgauer, P., Sigmund, W., Kadach, D., Stahl, K., 2017, *Comprehensive simulation methods for crossed helical gear sets with the main focus on the calculation of contact patterns*, Forsch Ingenieurwes, 81, 299–306.
14. Liang, D., Meng, S., Tan, R., 2021, *Mathematical model and characteristics analysis of crossed-axis helical gear drive with small angle based on curve contact element*, Science progress, 104(2), pp. 1-19.
15. Octrue, M., 2014, *Evolution of Worm Gear Standards and their Consequences on Load Capacity Calculation Approach*, Power Transmission Engineering, 6, pp. 36-42.
16. Chernets, M.V., 2019, *Prediction Method of Contact Pressures, Wear and Life of Worm Gears with Archimedean and Involute Worm*, Taking Tooth Correction into Account. J. Frict. Wear, 40, pp. 342–348.
17. Daubach, K., Oehler, M., Sauer, B., 2021, *Wear simulation of worm gears based on an energetic approach*, Forsch Ingenieurwes.
18. Ivanov, A.S., Goncharov, S.Y., 2021, *Wear and Efficiency of Worm Gears with Running-In*. Russian Engineering Research, 41(8), pp. 697–700.
19. Weisel, C., 2018, *Einfluss der Tragbildgröße und –lage auf den Wirkungsgrad und den Betriebsverschleiß bei Schneckengetrieben*, FVA-Heft Nr. 853.
20. Miltenović, A., Nikolić, V., Banić, M., 2015, *Wear Load Capacity of Crossed Helical Gears with Wheel Made from Sintered Steel*, Science of Sintering, 47, pp. 153-163.
21. Miltenović, A., 2016, *Damage types, Load Capacity and Efficiency of Crossed Helical Gears with Wheels from Sintered Steel*, Theory and Practice of Gearing and Transmissions, Mechanisms and Machine Science, 34, pp. 189-232.
22. Miltenović, A., Nikolić, V., Milovančević, M., Banić, M., 2012, *Experimental and FEM analysis of sintered steel worm gear wear*, Transactions of FAMENA, 36(4), pp. 85-96.
23. Krol, O., Sokolov, V., 2022, *Optimal Choice of Worm Gearing Design with Increased Wear Resistance for Machine's Rotary Table*, Advanced Manufacturing Processes III, InterPartner 2021, Lecture Notes in Mechanical Engineering, Springer, pp. 3-12.
24. Predki, W., Miltenović, A., 2010, *Influence of Hardening on the Microstructure and the Wear Capacity of Gears made of Fe1.5Cr0.2Mo Sintered Steel*, Science of Sintering, 42, pp. 183-191.